Journal of Environmental Management 258 (2020) 110023

Contents lists available at ScienceDirect

Journal of Environmental Management

journal homepage: http://www.elsevier.com/locate/jenvman

Research article

A model to integrate urban river thermal cooling in river restoration

Reza Abdi [a,*], Theodore Endreny [b], David Nowak [c]

[a] Department of Civil and Environmental Engineering, Colorado School of Mines, Golden, CO, 80401, USA
[b] Department of Environmental Resources Engineering, State University of New York, College of Environmental Science and Forestry, Syracuse, NY, 13210, USA
[c] USDA Forest Service, Northern Research Station, 5 Moon Library, SUNY-ESF, Syracuse, NY, 13210, USA

ARTICLE INFO

Key Terms:
Los angeles river (LA river)
Sawmill creek (SM creek)
Urban river
Thermal pollution
Riparian shading
Green infrastructure

ABSTRACT

River water quality and habitats are degraded by thermal pollution from urban areas caused by warm surface runoff, lack of riparian forests, and impervious channels that transfer heat and block cool subsurface flows. This study updates the i-Tree Cool River model to simulate restoration of these processes to reverse the urban river syndrome, while using the HEC-RAS model water surface profiles needed for flood hazard analysis in restoration planning. The new model was tested in a mountain river within the New York City drinking water supply area (Sawmill, SM, Creek), and then used for base case and restoration scenarios on the 17.5 km reach of the Los Angeles (LA) River where a multi-million dollar riverine restoration project is planned. The model simulated the LA River average temperature in the base case decreased from 29.5 °C by 0.3 °C when warm surface inflows were converted to cooler groundwater inflows by terrestrial green infrastructure; by 0.7 °C when subsurface hyporheic exchange was increased by removal of armoring and installation of riffle-pool bedforms; by 3.6 °C when riparian forests shaded the river; and by 6.4 °C when floodplain forests were added to riparian forests to cool surface reservoirs and local air temperatures. Applying all four restoration treatments lowered river temperature by 7.2 °C. The simulated decreases in river temperature lead to increased saturated dissolved oxygen levels, reaching 8.7 mg/L, up from the 7.6 mg/L in the base case scenario, providing improved fish habitat and reducing eutrophication and hypoxic zones. This study evaluating the performance of environmental management scenarios could help managers control the thermal pollution in rivers.

1. Introduction

The "urban stream syndrome" describes the ecological degradation of waters draining urban lands and is characterized by a rapid oscillation in water flows (i.e., flashy hydrographs; Mazrooei et al., 2017), increased nutrient and metal concentrations, straightened and flattened channel banks and bed (i.e., channelized), reduced biotic richness (Walsh et al., 2005; Abdi and Yasi, 2015), and thermal pollution, characterized by hot urban surfaces (i.e., urban heat island) generating water temperatures above the tolerance of native fauna (Somers et al., 2013). To remediate the urban stream syndrome, urban areas could naturalize stormwater management (Walsh et al., 2005) and reduce the urban heat island, which typically involves the restoration of floodplain and riverine urban areas (Somers et al., 2013; Shafiei Shiva et al., 2019), which typically require flood hazard area development permits (Ohio EPA, 2019).

The ecological impacts of urban river degradation, overall, are extensive and have been the focus of work by scientists, city planners, and policymakers (Somers et al., 2013; Grizzetti et al., 2017; Cai et al., 2019). There are large economic benefits in reducing river temperature (Seedang et al., 2008), which stem from increasing riverine dissolved oxygen (DO), reducing harmful algal blooms (Anderson et al., 2000), and slowing accelerated eutrophication from nutrient loading (Pretty et al., 2003; Nguyen et al., 2019). Riverine thermal pollution changes riverine ecology by directly and indirectly affecting the metabolism of living organisms, their food webs, and their habitat suitability (Gitay et al., 2002; Stefan and Sinokrot, 1993; Logan and Stillwell, 2018). Dodds et al. (2009) estimated the damage costs of accelerated eutrophication in the freshwater of the USA at approximately $2.2 billion per year, while Pretty et al. (2003) estimated the cost in England and Wales at $105–160 million per year. Total maximum daily loads as quantitative thresholds for thermal pollutant sources (Seedang et al., 2008) are established to address river degradation due to thermal pollution (US EPA, 2013).

Naturalization of stormwater management and reduction of the urban heat island can be part of holistic plan replacing terrestrial and

* Corresponding author.
E-mail address: rabdi@mines.edu (R. Abdi).

https://doi.org/10.1016/j.jenvman.2019.110023
Received 22 July 2019; Received in revised form 10 December 2019; Accepted 20 December 2019
Available online 6 January 2020

aquatic grey infrastructure with green infrastructure. Terrestrial grey infrastructure, such as buildings, parking lots, and roads, warms air temperatures and conveys stormwater to gutters and sewers (Somers et al., 2013), and aquatic grey infrastructure, such as bridges and concrete embankments, channelizes and removes nature form the rivers. Terrestrial green infrastructure, such as bioretention basins and bioswales, increase canopy interception and storage of precipitation, soil infiltration rates, plant and soil evapotranspiration, solar shading of runoff, and surface roughness thereby slowing runoff and reducing riverine flooding (US EPA, 2016; Mosleh and Zamani-Miandashti, 2013).

Aquatic green infrastructure, such as riparian vegetation, permeable riverbeds and banks, and in-channel bedform morphology, increases habitat and shading in the aquatic ecosystem, reduces erosion, and induces cooling groundwater inflow and hyporheic exchange (Bernhardt et al., 2005; USDA-NRCS, 2007; Greenway, 2017; Giner et al., 2019). Hyporheic exchange describes the mixing of surface and shallow subsurface water in the hyporheic zone, which is the porous region surrounding the river bed (Crispell and Endreny, 2008). Eco-hydrologists encourage the restoration of hyporheic exchange through the removal of impervious channels and reshaping bedform morphology with riffle-pool and meander sequences (Hester and Gooseff, 2010). River basin restoration can be managed for the multiple goals of flood control and improved water quality important for human wellbeing and biodiversity (European Commission, 2013; Izadmehr and Rockne, 2018).

The federal and industry standard for reengineering floodplain and riverine urban areas and associated flood hazard analysis is the US Army Corps of Engineers (USACE) Hydrologic Engineering Center River Analysis Software (HEC-RAS) model (FEMA, 2019). The HEC-RAS model has limits with respect to ecological restoration. In the case of thermal restoration, while it simulates river temperature, it neglects the role of riparian shade, substrate, and groundwater-surface water exchange (e.g., hyporheic fluxes) when simulating river temperature, making it difficult to assess whether restoration achieved thermal pollution and flood hazard goals. To create a more holistic model package, we created a set of functions that incorporate HEC-RAS model outputs of river water surface profiles, designed for flood hazard mapping, into the i-Tree Cool River Model (Abdi and Endreny, 2019), designed for ecological restoration. This model package can then simulate how river basin naturalization affects thermal pollution and flood hazard goals (Armal et al., 2018).

The present study aims to improve river restoration management by creating and testing functions that incorporate HEC-RAS model outputs of river water surface profiles into the i-Tree Cool River Model that simulates nature-based cooling of waters (Abdi and Endreny, 2019). The i-Tree Cool River model (Abdi and Endreny, 2019) updates maintain the HEC-RAS model water surface profiles and allow for inflows of cool groundwater inflows from terrestrial green infrastructure (e.g. bioretention or infiltration trench), riverine shading from riparian trees, and hyporheic exchange in a permeable riverbed. The science question: How much is the thermally polluted LA River potentially cooled by riverine shading, hyporheic exchange, and subsurface inflows? Each model operates by simulating the water and energy balance in reach segments between river cross-sections. The study provides the i-Tree Cool River model as freeware to plan and design the thermal restoration, while optionally using river water surface profile data for flood hazard methods.

2. Methods

2.1. Study areas

This study analyzed two watersheds. The first watershed was a 2 km reach of Sawmill (SM) Creek draining a 15 km^2 watershed in Tannersville, New York (Fig. S1 [1]). The SM Creek is a second-order mountainous river with varying watershed land use, starting in forests and transitioning to urban land (See Fig. S2; Abdi and Endreny, 2019).The second watershed included 0.5 and 17.5 km reaches of the Los Angeles (LA) River draining a 1270 km^2 watershed in LA, California (Figs. 1 and S3). At present, the LA River for the 82 km upstream of its discharge at the Port of Long Beach is predominantly concrete armored with uniform geometry to expedite stormwater removal and provide flood protection (Read et al., 2019; Mika et al., 2017; See Fig. S4). The LA River reach situated between Griffith Park and downtown LA is notable for its channelized trapezoidal cross-section form, concrete armoring, lack of riffle-pool bedform morphology, and lack of riparian vegetation. This LA River reach is part of the multi-million dollar Los Angeles River Ecosystem Restoration Project managed by the US Army Corps of Engineers (USACE) in partnership with the City of LA (USACE, 2019).

2.2. Model equations

The model used for these simulations is an updated version of i-Tree Cool River model (Abdi and Endreny, 2019). This model was updated to include HEC-RAS model river water surface routines. The i-Tree Cool River model uses standard advection, dispersion, and reaction equations to simulate the water transport and a change in water temperature between two cross-sections. River temperature is estimated as (Abdi and Endreny, 2019):

$$T = T^{t-1} + \Delta t\left[V\frac{T_{up} - T}{\Delta x} - D_L\frac{T_{up} - 2T - T_{dn}}{(\Delta x)^2}\right] + R_h + R_i \quad (1)$$

where T (°C) is the temperature at a river cross-section, the superscript *t-1* indicates the prior time, Δt (s) is the time step, the subscript *up* indicates the upstream cross-section, the subscript dn indicates the downstream cross-section, V (m/s) is the cross-section velocity, Δx (m) is the length of the reach segment bounded by the cross-section and upstream cross-section, D_L (m^2/s) is the reach longitudinal dispersion computed as a function of cross-section velocity and depth, R_h (°C) is the loss or gain (i.e., reaction term) of temperature due to heat flux, and R_i (°C) is the loss or gain of temperature due to lateral inflows (Abdi and Endreny, 2019, USACE 2016). The velocity is determined by a separate set of hydraulic equations, which in steady-state mode involves simultaneously estimating depth and velocity to satisfy the conservation of energy, mass, and momentum, i.e., the 5-step algorithm used in HEC-RAS (USACE, 2016), which is now an alternative to the Newton-Raphson algorithm used in i-Tree Cool River (see supplementary materials section S1, Abdi and Endreny, 2019).

The heat flux reaction term is defined as:

$$R_h = \frac{\varphi}{\rho \cdot C_p \cdot y} \quad (2)$$

where ϕ (W/m^2) is heat flux at the cross-section and represents the heat flux within the adjacent upstream reach segment, ρ (kg/m^3) is water density, C_p (J/kg/°C) is specific heat of water, and y (m) is water depth at the cross-section (Abdi and Endreny, 2019, USACE, 2016). For HEC-RAS, ϕ is the combined terms of shortwave energy flux from solar radiation, longwave energy flux from atmospheric temperature radiation, longwave energy flux from river temperature radiation, latent heat flux from wind entraining river evaporation, and sensible heat flux from wind entraining river temperature. For i-Tree Cool River, ϕ includes the above HEC-RAS terms, as well as: a) additional parameters in the shortwave radiation and atmospheric longwave radiation calculations to represent the effects of trees, hills and buildings on receiving and emitting radiation via shade and view to sky factors, and b) additional

[1] Figures with "S" are presented in the supplementary materials.

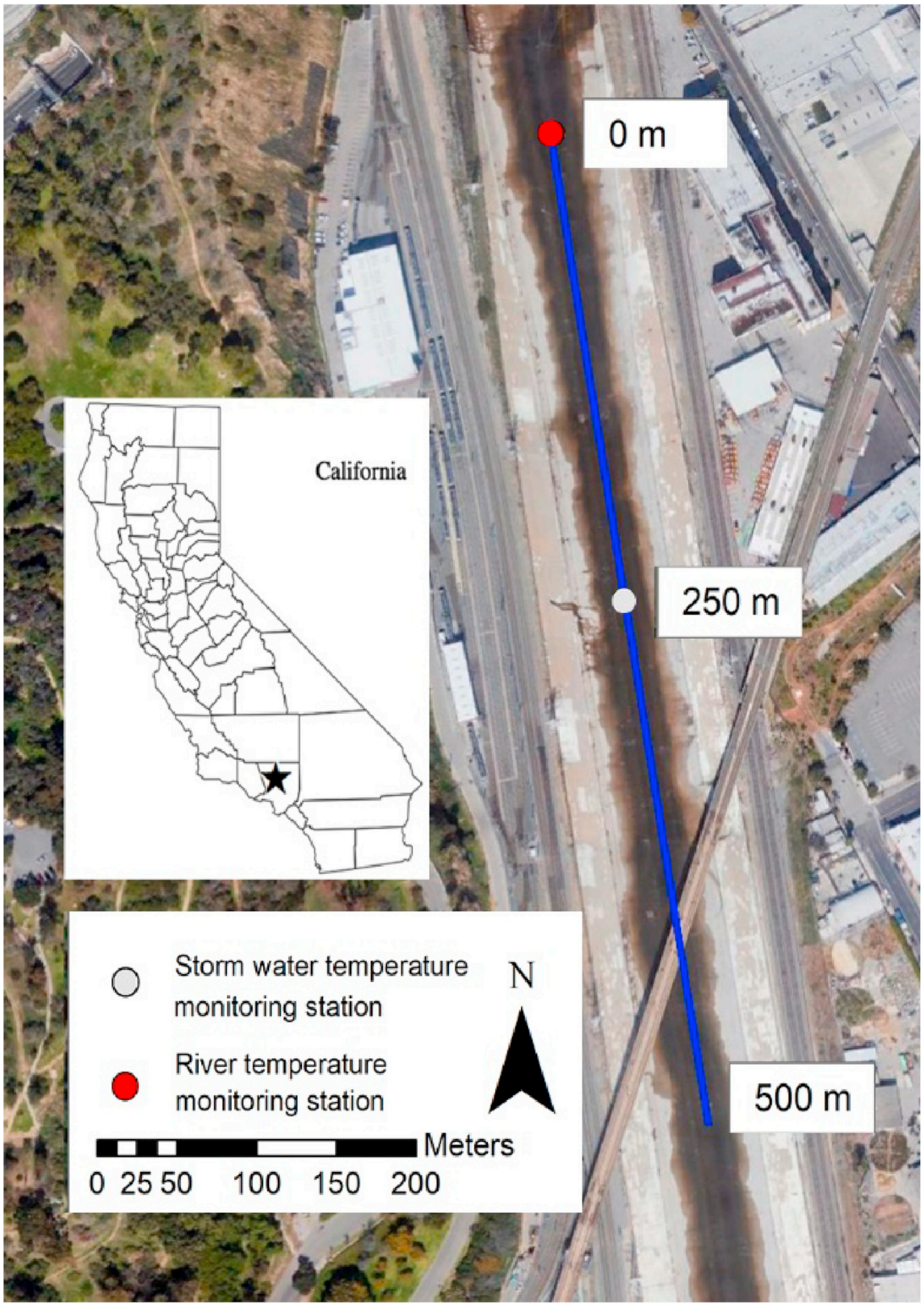

Fig. 1. The monitoring station of the LA River upstream boundary cross-section and a surface water inflow location. The inset with star shows the site location within the state of California.

flux terms for vegetation longwave radiation and riverbed substrate radiation (Abdi and Endreny, 2019) (Fig. 2).

The lateral inflow reaction term is defined as:

$$R_i = \frac{Q_{up}T_{up} + Q_aT_a + Q_bT_b + Q_cT_c}{Q_{up} + Q_a + Q_b + Q_c} - T_{up} \quad (3)$$

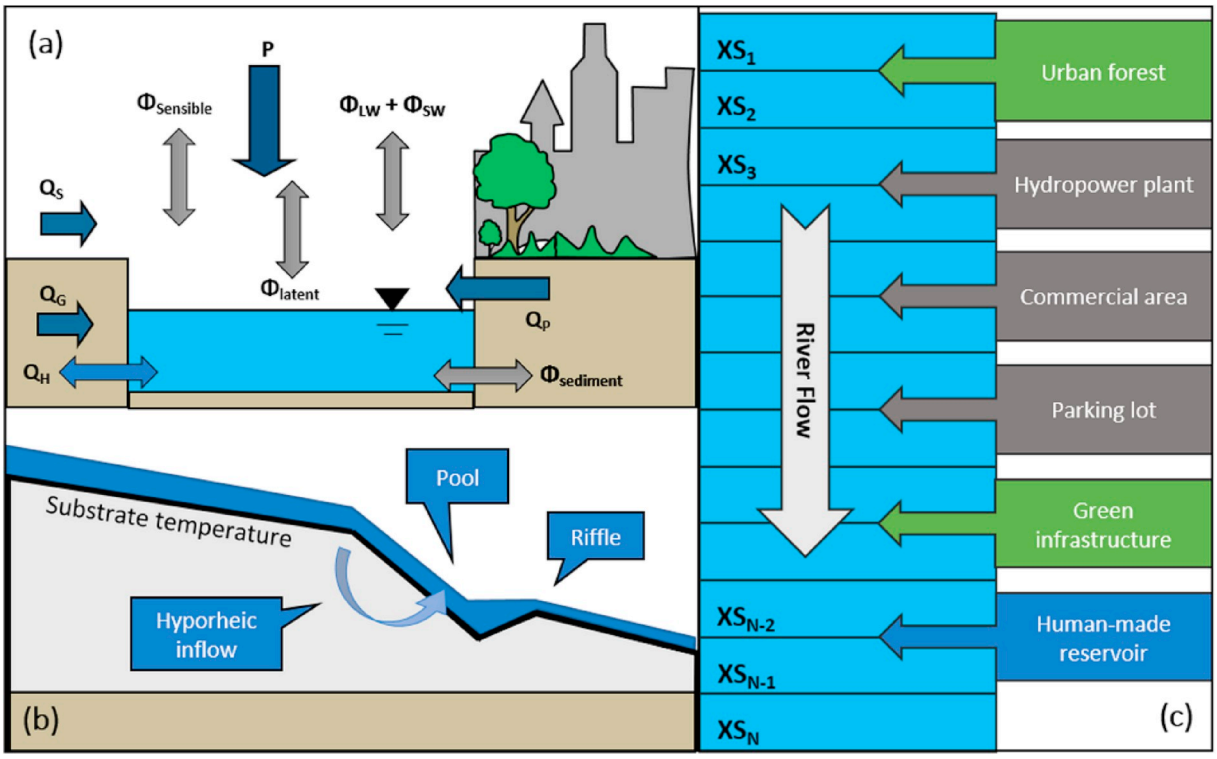

Fig. 2. Schematics of the i-Tree Cool River model: (a) River cross-section view, demonstrating the energy and water balances. In this figure, *P* represents precipitation, and Q_S, Q_G, and Q_P represent the surface flow, groundwater flow, and pipe flow, respectively. Φ is the heat flux, and subscripts $_{LW}$ is longwave radiation flux, $_{SW}$ is shortwave radiation flux, $_{latent}$ is latent heat flux, $_{sensible}$ is sensible heat flux, and $_{sediment}$ is bed sediment heat flux; (b) River longitudinal section for a riffle-pool bedform. The hyporheic inflow pathways around the riffle-pool and substrate temperature are shown in the panel; and (c) River plan view demonstrating the potential lateral inflows that can be added to the river flow in either dry or wet weather. *XS* represents the cross-section of the river reach.

where Q (m^3/s) is the discharge, T (°C) is the temperature, and subscripts a, b, and c represent separate inflows to that segment; there is no maximum number of inflows, but the minimum number of inflows is 0 ($R_i = 0$). For HEC-RAS, only lateral inflows of tributaries are simulated, while i-Tree Cool River simulates lateral inflows of tributaries, groundwater, and hyporheic exchange. The groundwater inflow is assigned to each cross-section based on hydrological analysis or differencing the upstream and downstream flow rates, while hyporheic exchange flux is auto-computed by the model as a function of the local substrate conductivity and hydraulic gradient between cross-sections (see Eq S(1) in Abdi and Endreny, 2019).

To combine the i-Tree Cool River model simulation of green infrastructure impacts on temperature with the HEC-RAS model simulation of water surface profiles, Eq (1) was modified to include the velocity and discharge data from the HEC-RAS model. The retention time was added to the equation in order to apply the HEC-RAS model calculated velocity data.

$$T = \frac{\left[T_{up}^{t-1} + \Delta t_r R_{h2}\right] Q}{Q} + \frac{R_{i2}}{Q} \tag{4}$$

where T_{up}^{t-1} is the temperature of the upstream cross-section at the prior time step, Δt_r (s) is the retention time step defined as $\Delta t_r = \Delta x / V$ and V (m/s) is the HEC-RAS velocity at the cross-section, Q (m^3/s) is the HEC-RAS discharge at the cross-section, and R_{h2} is the heat flux reaction term, and R_{i2} is lateral inflows reaction term. An updated heat flux reaction term is needed for Eq (4),

$$R_{h2} = \left[\frac{\varphi}{\rho \cdot C_p \cdot y} - D_L \frac{\left(\frac{\varphi}{\rho \cdot C_p \cdot y \cdot V} - \frac{\varphi_{up}}{\rho \cdot C_p \cdot y_{up} \cdot V_{up}}\right)}{\Delta x}\right] \tag{5}$$

where ϕ is defined to include the i-Tree Cool River model tree-based terms (for more detail, see equation (4) of Abdi and Endreny, 2019). An updated lateral inflows reaction term is needed for Eq (4),

$$R_{i2} = \frac{Q_a T_a + Q_b T_b + Q_c T_c}{Q_a + Q_b + Q_c} \tag{6}$$

where subscripts a, b, and c are defined as the i-Tree Cool River form with Eq (3) above.

This study updated i-Tree Cool River model to utilize water surface profile data from the HEC-RAS model and thereby coordinate evaluations of thermal and flood management impacts. By coupling the hydraulic transport model of HEC-RAS with the temperature transport model of i-Tree Cool River, Eq (4) can lead to differences in the volume of water predicted by the two transport models. This difference is due to the first right hand side term in Eq (4) representing temperature transport as plug flow, with upstream temperature from the prior time step replacing downstream temperature in the current time step, even when upstream and downstream volumes may not be equal for each reach segment. To avoid this continuity error, the i-Tree Cool River model maintains the HEC-RAS model volume for each reach segment, and uses cross-section spacing of 5 m or less to constrain the error in the temperature estimate.

2.3. Model inputs and scenarios

The updated i-Tree Cool River model was run in steady state, defined as $dQ/dt = 0$, and non-uniform conditions, $dQ/dx \neq 0$, where Q is discharge, t is time (s), and x is river distance (m). This approach keeps the water surface profile constant through time at all locations and allows it to vary with location due to groundwater and other inflows, which is a standard process for flood hazard analysis (USACE, 2016).

2.3.1. Sawmill creek

The simulation of the 2 km reach of Sawmill (SM) Creek on July 2 and 3, 2007 received 0.1 m^3/s baseflow discharge at the upstream boundary cross-section (river station 0 m), then received urban drainage via storm sewers at cross-sections 620 m and 790 m, and lastly received retention basin discharge at cross-section 1450 m. Storm sewer flows were estimated using stage-discharge relations, monitoring stage with pressure transducers (manufactured by Global Water Instruments). Stage data was converted to discharge using the Manning equation, with stage converted to channel area and hydraulic radius using geometry relations, and the Manning roughness coefficients estimated from pebble counts at each cross-section by Crispell (2008). The alternative scenarios for the SM Creek are: a) simulating the system without the cooling effect of the subsurface inflow, b) deactivating the warming effect of the lateral inflows from the urban drainage and retention basin, and c) simulating the river temperature with estimated upstream river temperature boundary conditions in place of the observed upstream river temperature boundary condition.

The importance of the effective stressors impacting the alternative scenarios was demonstrated by modifying the key parameters in the i-Tree Cool River model. The role of these parameters in the defined alternative scenarios is presented in the results section and the supplementary materials. In the simulations, the cross-section data needed by the HEC-RAS model were obtained for the SM Creek from field surveys (Crispell, 2008). In the base case scenario for SM Creek, the upstream boundary condition and lateral inflow temperature time series in cross-sections 620 m, 790 m, and 1450 m were obtained from observed hourly data (Crispell, 2008). Inputs of hourly weather data including the direct normal irradiance (DNI) and diffuse horizontal irradiance (DHI) shortwave radiation as well as air temperature and relative humidity for SM Creek were obtained from the National Solar Radiation Data Base (NSRDB), at station ID #1227776. The groundwater temperature was set as a function of the annual average air temperature as recommended in the literature (Glose et al., 2017), at 13 °C for SM Creek base case and alternative scenarios.

2.3.2. Los Angeles River

The simulation of the Los Angeles (LA) River was for June 17 and 18, 2016 for reach lengths of 0.5 and 17.5 km, each with no riparian forest, no riffle-pool bedform and warm surface inflows entering at cross-section 250 m. These base cases were estimated by U.S. Geological Survey StreamStats (U.S. Geological Survey, 2016) to receive 4.34 m^3/s baseflow discharge at the upstream boundary cross-section (0 m). The alternative scenarios for the LA River simulated: a) infiltrating tertiary treated wastewater flows of 0.8 m^3/s (Mongolo et al., 2017) into green infrastructure so it entered the reach as cool groundwater inflow rather than warm surface inflow at cross-section 250 m; b) replacing the featureless channel bottom with riffle-pool bedform morphology to increase hyporheic exchange; c) replacing the bare concrete channel banks with riparian forest to increase shade and reduce substrate and water temperature; and d) expanding the floodplain forest in the LA residential area from 12.1% cover to the potential of 36% cover to cool the air and upstream water temperature, and shade upstream reservoirs. The specific characteristics of the alternative scenarios implemented in the i-Tree Cool River model are summarized in Table 1 and Table S1. The floodplain forest is defined as any forest extending from the riparian area into the greater watershed, and for this scenario it extended upstream of the study reach. The potential forest cover is the existing forest cover combined with new forest cover that extends into suitable planting areas, and was inventoried for LA by Endreny et al. (2017).

The analysis was conducted by first running the HEC-RAS model to generate water surface profile data, then running the i-Tree Cool River model with Eqs (4)–(6) in place of Eqs (1)–(3). The cross-section data needed by the HEC-RAS model were obtained for the LA River from document analysis of channel geometry and photo interpretation of channel base width (Mongolo et al., 2017; USACE, 2015). The HEC-RAS model provided the water surface profile outputs needed by the i-Tree Cool River model for each cross-section: x (m); discharge, Q (m^3/s); minimum channel elevation (m) and water surface elevation (m) used to compute flow depth, y (m); velocity in channel, V (m/s); top width, w (m), flow area (m^2); and wetted perimeter (m). The i-Tree Cool River model resamples HEC-RAS outputs with linear interpolation to refine the spacing of cross-sections to 5 m or finer and resolve spatial variation channel and riparian features and reduce inconsistencies between temperature and hydraulic transport in Eq (1).

The i-Tree Cool River model uses the resampled HEC-RAS outputs along with the boundary condition temperatures, radiation fluxes, shading, substrate, and other features affecting river temperature estimates. For the LA River hourly temperature data did not exist, and base case data were generated using a two-step process: 1) applying a non-linear regression (Mohseni et al., 1998) transforming hourly air temperature into river temperature, with air temperature from nearby Burbank Airport station, and regression coefficients of $\alpha = 32.48$, $\beta = 15.18$, and $\gamma = 0.17$ (Eq (7); Fig. S5); and 2) applying a linear regression transforming the 1st estimate to match observed June river temperature statistics at the upstream boundary, with slope 1.206 and intercept 1.665 determined from the linear regression between the minimum and maximum river temperatures from observed June 2016 data (Mongolo et al., 2017) and the 1st estimate of river temperature (see Fig. S6). This linear regression was used to match inflow temperatures not predicted by the non-linear regression with air temperature is presumed to account for the urban heat island impact, including warm surface inflows from tertiary treated wastewater in upstream lakes (e.g., the Japanese Garden Lake and Balboa Recreation Lake) noted by Mongolo et al. (2017). Inputs of hourly weather data including the DNI and the DHI shortwave radiation for the LA River were obtained from the NSRDB, at station ID #81603. A look-up table was used for calculating the dissolved oxygen concentration at saturation as a function of freshwater temperature (www.lakestewardsofmaine.org).

$$T_W = \mu + \frac{\alpha - \mu}{1 + e^{\gamma(\beta - T_{air})}} \tag{7}$$

The groundwater temperature was set as a function of the annual average air temperature, at 20 °C for the LA River base case and restoration scenarios. The LA River scenario with floodplain forest expansion was estimated to cool the June 17–18, 2016 air temperatures due to

Table 1
The i-Tree Cool River inputs of average temperature for air, groundwater, upstream boundary condition, substrate, and surface runoff for the base case and restoration scenarios. The table also demonstrates the saturated dissolved oxygen (Sat. DO) level corresponded with the temperature.

System Component	Scenarios					
	Full Sun (No riparian or floodplain forest expansion)		Riparian Forest (No floodplain forest expansion)		Riparian Shade and Floodplain Forest Expansion	
	Temperature (°C)	Sat. DO (mg/L)	Temperature (°C)	Sat. DO (mg/L)	Temperature (°C)	Sat. DO (mg/L)
Air	23.7	8.5	23.7	8.5	21.5	8.8
Groundwater	20.0	9.1	20.0	9.1	20.0	9.1
Boundary conditions	28.6	7.7	28.6	7.7	25.1	8.2
Substrate	32.0	7.5	32.0	7.5	27.0	8.0
Surface runoff	30.0	7.6	30.0	7.6	30.0	7.6

evapotranspiration, simulated by i-Tree Cool Air (Yang et al., 2013). These scenario air temperatures, with an average of 21.5 °C (2.2 °C cooler than the base case), were used in the non-linear regression of Mohseni et al. (1998) to estimate new river temperatures, with an average of 25.1 °C, which represented mitigation of the urban heat island (see Table 1). The LA River riparian forest scenario was estimated to increase the shade factor from 0, no shade, to 1, full shade, and cool June 17–18, 2016 average river substrate temperature from 32 °C to 27 °C, based on analysis of daily average June to August river corridor temperatures provided by Weng and Fu (2014). Details on other i-Tree Cool River model inputs used to simulate temperature are provided in the supplementary materials section S1, and a manual and sample inputs can be downloaded at http://www.itreetools.org/research_suite/coolriver/.

3. Results

3.1. The SM creek

The simulated and observed average river temperature for SM Creek was 13.8 °C, and spatial and temporal variation in that temperature was used for validation of the i-Tree Cool River model; the model was not calibrated to the observed data. The temporal pattern in simulated and observed reach-averaged river temperature captured the sinusoidal heating and cooling due to diurnal variation in radiation, with additional temporal variation due to cloud cover, and wind (Fig. S7). The model simulation underestimated the observed variation in river temperature by 0.85 °C, split between overestimating the nighttime minimum and underestimating the daytime maximum temperature. The spatial performance of the i-Tree Cool River model in SM Creek was assessed against observed data at 12 cross-sections, with water entering the reach at 12.5 °C and warming by 3.6 °C due to lateral inflows, primarily from a surface reservoir. At the upstream boundary, the model used observed values and hence had a perfect coefficient of determination R^2 of 1 (Fig. S8), and at the other 11 locations the smallest R^2 was 0.8, the largest R^2 was 0.95, and the average R^2 was 0.88. This analysis of steady flow extends the work by Abdi and Endreny (2019) on unsteady state flows in SM Creek. To validate the model, a Nash-Sutcliffe Efficiency (NSE) metric was used to assess the goodness of fit between observed and simulated reach-average time series, achieving an NSE of 0.93, close to the perfect NSE of 1. The simulated vs observed time series had a coefficient of determination R^2 of 0.95, and a root mean square error (RMSE) of 0.1 °C. A statistical *t*-test of the time-averaged observed and simulated temperature time series having no meaningful difference, with an $\alpha = 0.05$, had a p-value of 0.90, showing there was no meaningful difference between the simulated and observed temperatures. To understand the role of different drivers of urban river temperature to guide the LA River restoration scenarios presented in section 3.2, an analysis using the i-Tree Cool River model and based on the alternative scenarios was conducted to confirm the importance of cool groundwater inflow and hyporheic exchange, warm surface water inflows, and a cool upstream boundary condition (Fig. S9). The effective parameters for each scenario are explained in the supplementary materials (see the section for Fig. S9).

3.2. The LA river

The simulated river temperature in the LA River for the base case 0.5 km reach length had an average river temperature of 28.7 °C, with a diurnal pattern of warming and cooling (Fig. 3), and the average temperature rose by 0.05 °C per km to 29.5 °C at the 17.5 km reach length (see Table 2). The average river temperature associated with each restoration scenario was then subtracted from the base case river temperature at the equivalent reach length to generate the cooling, noted as ΔT in Table 2. The paired-samples *t*-test with $\alpha = 0.05$ showed significant differences ($p < 0.05$) between simulated average river temperatures for each scenario and those of its 0.5 or 17.5 km reach length base case. The scenario of using green infrastructure inflows of infiltrated treated wastewater entering the river at groundwater temperature generated a ΔT of 0.3 °C from the 17.5 km reach base case (Table 2). The scenario of using riffle-pool bedform morphology to increase hyporheic exchange generated a ΔT of 0.7 °C from the 17.5 km reach base case. Combining the restoration treatments of green infrastructure and riffle-pool bedforms generated a ΔT of 0.9 °C from the 17.5 km reach base case, with the simulated average water temperature still increasing by 0.01 °C per km of reach due to the absence of riparian forest and full solar exposure on the river. Combining the restoration treatment of riparian shade with the restoration of green infrastructure and riffle-pool bedforms generated a ΔT of 4.4 °C from the 17.5 km reach base case, with the simulated average water temperature now decreasing by 0.17 °C per km of reach.

The single scenario of riparian shade generated a ΔT of 3.6 °C from the 17.5 km reach base case, with average water temperature decreasing by 0.14 °C per km of reach when cooling was not provided by the riffle-pool hyporheic exchange and green infrastructure induced groundwater inflows. Combining the four restoration treatments of floodplain forests

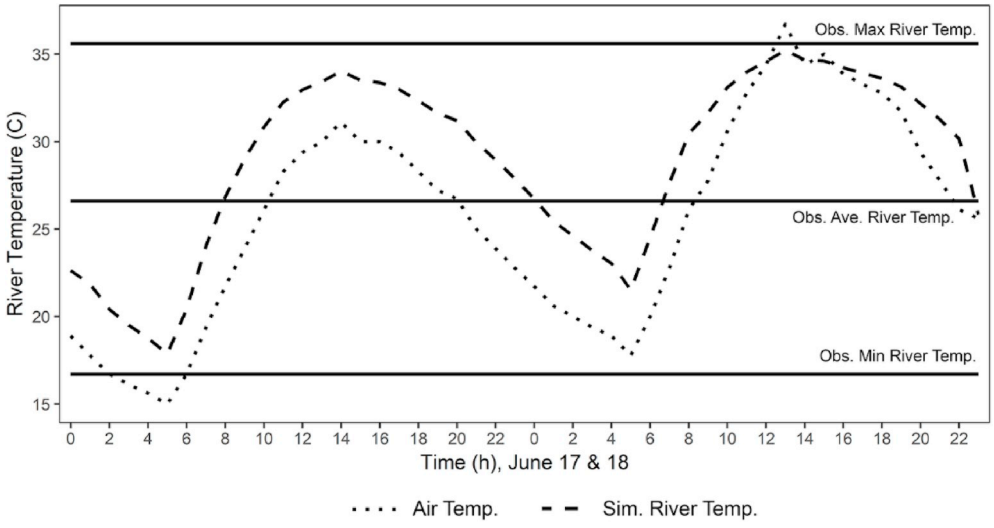

Fig. 3. The hourly observed air temperature and simulated river temperature in the LA River for June 17 to 18, 2016 with the observed average, minimum, and maximum river temperatures for the month of June.

Table 2
The i-Tree Cool River model simulated average river temperature (°C) in the 0.5 and 17.5 km reach lengths of the LA River for base case and all scenarios, and the temperature differences (°C) between each scenario and the base case for the same reach length row. In the table, *GI* stands for scenarios with green infrastructure and *NO GI* stands for scenarios without green infrastructure.

Reach length (km)	Var. (°C)	Full Sun (No riparian or floodplain forest expansion)				Riparian Shade (No floodplain forest expansion)				Riparian Shade and Floodplain Forest Expansion			
		No Riffle-Pools		With Riffle-Pools		No Riffle-Pools		With Riffle-Pools		No Riffle-Pools		With Riffle-Pools	
		No GI	GI	No GI	GI	No GI	GI	No GI	GI	No GI	GI	No GI	GI
0.5	T	28.7	28.6	28.5	28.4	28.3	28.2	28.1	28.0	25.2	25.1	25.0	24.9
	ΔT	0.0	0.1	0.2	0.3	0.4	0.5	0.6	0.7	3.5	3.6	3.7	3.8
17.5	T	29.5	29.2	28.8	28.6	25.9	25.7	25.4	25.1	23.1	22.9	22.5	22.3
	ΔT	0.0	0.3	0.7	0.9	3.6	3.8	4.1	4.4	6.4	6.6	7.0	7.2

with riparian shade, terrestrial green infrastructure, and riffle-pool bedforms generated the largest ΔT of 7.2 °C from the 17.5 km reach base case, 64% cooler than the ΔT of 4.4 °C when riparian shade, green infrastructure, and riffle-pool bedforms were combined. The combination of 4 restoration treatments caused average water temperature to decrease by 0.15 °C per km of reach. The impact of the floodplain forest scenario cools the upstream boundary river temperature, and when combined with the riparian forest this cooler water propagates down river. This is evident in the 0.5 km reach when comparing the ΔT of 3.5 °C for the scenario with only riparian shade and floodplain forest and ΔT of 0.7 °C for the scenario combining treatments of riparian shade, green infrastructure, and riffle-pool bedforms.

The simulated cooling of the LA River temperature by the restoration scenarios led to the potential for higher saturated DO levels (Fig. 4). The percent difference between the average DO associated with each base case and restoration scenario, relative to the base case at the equivalent reach length of 0.5 or 17.5 km, was used to compute the ΔDO (%). The lowest DO saturation was 7.6 mg/L for the 17.5 km reach base case, and the highest DO saturation was 8.7 mg/L for the 17.5 km reach with all four treatments. The restoration scenarios without riparian shade on the 17.5 km reach had an average ΔDO_{sat} of 2% (Fig. 4). The scenario of riparian shade as the only restoration treatment increased the ΔDO_{sat} to 6%, and the combination of riparian shade, green infrastructure, and riffle-pool bedforms increased the ΔDO_{sat} to 8%. The scenario of floodplain forests increased the ΔDO_{sat} to 12.5%, while the combination of all 4 restoration treatments increased the ΔDO_{sat} to 14.5%. The error bars about the ΔDO_{sat} values represent uncertainty in model view-to-sky factors, generating ±0.2 °C variation in river temperatures, which led to 0.08–0.12 mg/L variation in DO_{sat} and a ±0.5% to ±1.6% error bar, with smaller values for the lower percentages.

4. Discussion

The reduction in warm water inflows at the upstream boundary and along the reach was a major contribution to the cooling of the LA River in simulations by the i-Tree Cool River model, an outcome supported by field observation and prior model development. The adverse thermal impacts of warm surface inflows was observed in the cool mountain area of SM Creek in NY when a lateral reservoir inflow caused a 2.4 °C warming of river temperature, the greatest warming along the reach (see Figs. S3 and S5). In the South Fork Yuba River of California, selective withdrawal from deeper, cooler layers within reservoirs is the recommended strategy to decrease summer river temperatures (Rheinheimer et al., 2015). The amount of cooling is a function of the relative volume and temperatures of the inflow compared with the river flow. Null et al. (2017) needed to increase the inflow of 21 °C reservoir water to 40% of

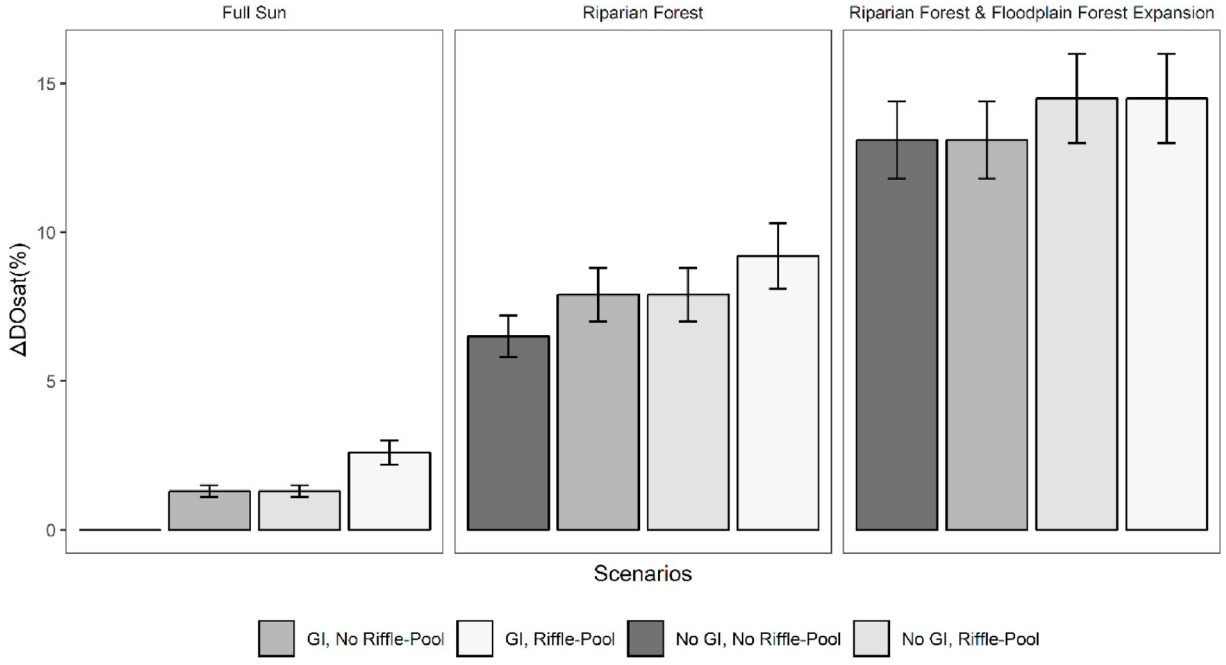

Fig. 4. The simulated average change (%) in saturated DO between the base case and all restoration scenarios for the 17.5 km reach of the LA River, June 17 to 18, 2016. The error bars show the uncertainty levels in the percentage of the ΔDO_{sat} associated with the view-to-sky factor. In the figure, *GI* stands for scenarios with green infrastructure and *NO GI* stands for scenarios without green infrastructure. (For interpretation of the references to colour in this figure legend, the reader is referred to the Web version of this article.)

the river flow during the 2015 summer in order to reduce >28 °C water temperatures on the East Walker River of Nevada by 5 °C and bring DO levels above 5 mg/L to reduce fish stress. Nichols et al. (2014) documented how cool groundwater inflows could mimic reservoir releases to lower the temperature of a Shasta River tributary in northern California, and how the unshaded tributary allowed this cool water to warm as it flowed downstream. This LA River simulations captured a similar phenomenon of groundwater cooling by redirecting warm surface inflows to infiltration, which then entered the river as 20 °C groundwater inflows. These inflows were 18% of the river's flowrate in the first 0.5 km section, which led to a decrease in the average LA River temperature of 0.3 °C. Similarly, the hyporheic exchange along the reach replaced warm river water with cool groundwater and had larg cooling effect in the LA River. Loheide and Gorelick (2006) noted the importance of hyporheic exchange in Cottonwood Creek in northern California during summer warm weather, and simulated how its absence led to river temperatures warming in the downstream direction. For the LA River, the restoration of riffle-pool bedforms will induce hyporheic exchange and replacement of 10% of the warm river water with cooler groundwater, lowering average river temperatures by 0.7 °C. Without proper watershed coordination, groundwater inflows can decrease. Risley et al. (2010) document how the pumping of wellfields reduced groundwater inflows to a river by 18% and caused summer river temperatures to warm by 0.5 °C.

The urban heat island phenomena warms the surface and air of Los Angeles (Weng and Fu, 2014), and this can be mitigated with forest plantings (Endreny, 2018; Yang et al., 2013). In the LA River scenarios, the ambient air temperature was simulated to decrease by 2.2 °C as a result of establishing riparian and floodplain forest a restoration treatment, leading to a decrease in average river temperature of 6.4 °C for the 17.5 km reach demonstrating the applicability of the developed solution in decision making process as well (Kazak and Hoof, 2018). The restoration scenario of riparian shading as the only restoration treatment led to a decrease in average river temperature of 3.6 °C for the 17.5 km reach, which is a response supported by other studies. Ketabchy et al. (2019) used a watershed heat budget model to demonstrate urban forest expansion cooled July and August 2015 water temperature in Stoubles Creek, Virginia by 1.4 °C to help meet targets for native fish habitat. Roth et al. (2010) simulated how the loss of urban riparian forest along the Boiron de Morges River in Switzerland warmed August 2007 average maximum air temperature by 1.6 °C and river temperature by 0.7 °C. Sun et al. (2015) showed how observed and modeled peak river temperatures in Mercer Creek of Washington has decreased by 4 °C in reaches that had more riparian and floodplain forest.

Decreasing the river temperature in the LA River would improve the saturation DO level, and thereby lead to better habitat for desired fish and other aquatic organisms. Our LA River scenario of all 4 restoration treatments lowered river temperature by 7.2 °C, resulting in a 14.5% increase in DO_{sat} level, improving conditions for desired fishes. As of 2011, 83% of California's native inland fish were extinct or declining (Moyle et al., 2011), and Carter (2005) reports in southern California, cold-water fishes such as trout (Oncorhynchus mykiss) avoid areas with DO less than 5 mg/L; for trout eggs, DO levels below 11 mg/L will delay their hatching, and DO below 8 mg/L will impair young trout growth and lower their survival rates. Due to climate change, the warm season river temperatures in the Sierra Nevada of California are predicted to increase by up to 5.5 °C by 2100, resulting in a 10% decrease in DO levels (Ficklin et al., 2013). Lower DO levels are a major reason for the hypoxic system in the LA River estuary (Diaz and Rosenberg, 2008), likely caused by excess loading of nutrients from human activity (Booth, 2015). The model developed in this study can assist planners such as those involved in the LA River restoration, where restoration might include floodplain and riparian forests for wildlife habitat and riffle-pool bedform morphology to encourage native fish habitat (USACE, 2015).

5. Conclusions

In this study, an updated version of i-Tree Cool River model was created to assess thermal restoration using water surface profile data from the HEC-RAS model. The updated i-Tree Cool River model can help planners assess the thermal benefit of floodplain and riverine restoration that naturalizes the hydrologic cycle, using HEC-RAS model water surface profiles approved for flood hazard mapping. Various restoration scenarios were simulated on a 17.5 km reach of the LA River targeted for ecological restoration. Findings are summarized as:

- Groundwater inflows coming from surface inflows that had been infiltrated to green infrastructure decreased the average river temperature by 0.3 °C.
- Hyporheic exchange coming from riffle-pool bedforms decreased the average river temperature by 0.9 °C.
- Diminished shortwave radiation from riparian forests decreased average river temperatures by 3.6 °C.
- Lower air temperatures and upstream reservoir temperatures decreased the temperature of the river at its upstream boundary, and when combined with the 3 above restoration treatments decreased average river temperature by 7.2 °C.

Author contribution

Conceptualization, R.A. and T.E.; methodology, R.A. and T.E.; software, R.A.; validation, R.A., T.E. and D.N.; formal analysis, R.A. and T.E.; investigation, R.A. and T.E.; resources, R.A. and T.E.; data curation, R.A. and T.E.; writing-original draft preparation, R.A.; writing-review and editing, R.A.,T.E. and D.N.; visualization, R.A.; supervision, T.E.; project administration, T.E. and D.N.; funding acquisition, T.E. and D.N.

Funding

This research was supported by the USDA Forest Service Northern Research Station i-Tree grant No. 15-JV-11242308-114.

Declaration of competing interest

We declare that we have no conflicts of interest to disclose.

Acknowledgment

We would like to thank Omid Mohseni, Laura Lautz, Ning Sun, and Jill Crispell for explaining their models.

Appendix A. Supplementary data

Supplementary data to this article can be found online at https://doi.org/10.1016/j.jenvman.2019.110023.

References

Abdi, R., Endreny, T.A., 2019. Urban river temperature modeling of unsteady stormwater inflows and riparian shading. Water 11 (5), 1060.
Abdi, R., Yasi, M., 2015. Evaluation of environmental flow requirements using eco-hydrologic-hydraulic methods in perennial rivers. Water Sci. Technol. 72 (3), 354–363.
Anderson, D.M., Hoagland, P., Kaoru, Y., White, A.W., 2000. Estimated Annual Economic Impacts from Harmful Algal Blooms (HABs) in the United States. Woods Hole (MA). Department of Biology, Woods Hole Oceanographic Institution. WHOI-2000-11.
Armal, S., Devineni, N., Khanbilvardi, R.M., 2018. Trends in extreme rainfall frequency in the contiguous United States: attribution to climate change and climate variability modes. J. Clim. 31 (1), 369–385.
Bernhardt, E.S., Palmer, M.A., Allan, D.J., Alexander, G., Barnas, K., Brooks, S., Carr, J., Clayton, S., Dahm, C., Follstad-Shah, J., et al., 2005. Synthesizing river restoration efforts. Science 308, 636–637.
Booth, A., 2015. State of the bay report. Looking ahead: nutrients and hypoxia. Urban Coast. 5 (1), 190–193.

Cai, W., Li, Y., Shen, Y., Wang, C., Wang, P., Wang, L., Liu, L., 2019. Vertical distribution and assemblages of microbial communities and their potential effects on sulfur metabolism in a black-odor urban river. J. Environ. Manag. 235, 368–376.
Carter, K., 2005. The Effects of Dissolved Oxygen on Steelhead Trout, Coho Salmon, and Chinook Salmon Biology and Function by Life Stage. California Regional Water Quality Control Board (North Coast Region).
Crispell, J.K., 2008. Hyporheic Exchange Flow Around Stream Restoration Structures and the Effect of Hyporheic Exchange Flow on Stream Temperature. Master of science degree thesis. State University of New York, College of Environmental Science and Forestry, p. 63.
Crispell, J.K., Endreny, T.A., 2008. Hyporheic exchange flow around constructed in-channel structures and implications for restoration design. Hydrol. Process. 23, 1158–1168.
Diaz, R., Rosenberg, R., 2008. Spreading dead zones and consequences for the marine ecosystem. Science 5891, 926–929.
Dodds, W.K., Bouska, W.W., Eitzmann, J.L., Pilger, T.J., Pitts, L., Riley, A.J., et al., 2009. Eutrophication of U. S. freshwaters: analysis of potential economic damages. Environ. Sci. Technol. 43 (1), 12–19.
Endreny, T.A., 2018. Strategically growing the urban forest will improve our world. Nat. Commun. 9 (1), 1160.
Endreny, T.A., Santagata, R., Perna, A., De Stefano, C., Rallo, R.F., Ulgiati, S., 2017. Implementing and managing urban forests: a much needed conservation strategy to increase ecosystem services and urban wellbeing. Ecol. Model. 360, 328–335.
European Commission, 2013. Individual Natural Water Retention Measures (NWRM): Stream Bed Re-naturalization. European Commission, p. 11.
FEMA, 2019. Hydraulic numerical models meeting the minimum requirement of national flood insurance program. https://www.fema.gov/hydraulic-numerical-models-meeting-minimum-requirement-national-flood-insurance-program.
Ficklin, D.L., Stewart, I.T., Maurer, E.P., 2013. Effects of climate change on stream temperature, dissolved oxygen, and sediment concentration in the Sierra Nevada in California. Water Resour. Res. 49, 2765–2782.
Glose, A., Lautz, L.K., Baker, E.A., 2017. Stream heat budget modeling with HFLUX: model development, evaluation, and applications across contrasting sites and seasons. Environ. Model. Softw. 92, 213–228.
Greenway, M., 2017. Stormwater wetlands for the enhancement of environmental ecosystem services: case studies for two retrofit wetlands in Brisbane, Australia. J. Clean. Prod. 163, 91–100.
Giner, M.E., Córdova, A., Vázquez-Gálvez, F.A., Marruffo, J., 2019. Promoting green infrastructure in Mexico's northern border: the Border Environment Cooperation Commission's experience and lessons learned. J. Environ. Manag. 248, 109104.
Grizzetti, B., Pistocchi, A., Liquete, C., Udias, A., Bouraoui, F., van de Bund, W., 2017. Human pressures and ecological status of European rivers. Sci. Rep. 7, 205.
Gitay, H., Suárez, A., Watson, R., Dokken, D.K., 2002. Climate change and biodiversity. Intergov. Panel Clim. Chang. (IPCC) 24, 77.
Hester, E.T., Gooseff, M.N., 2010. Moving beyond the banks: hyporheic restoration is fundamental to restoring ecological services and functions of streams. Environmental Science & Technology 44 (5), 1521–1525.
Izadmehr, M., Rockne, K., 2018. Pocket Wetlands for Nutrient Removal in Tile-Drained Agriculture. Talk Session Presentation at World Environmental and Water Resources Congress (Minneapolis, MN).
Kazak, J.K., Hoof, J.V., 2018. Decision support systems for a sustainable management of the indoor and built environment. Indoor Built Environ. 27 (10), 1303–1306.
Ketabchy, M., Sample, D.J., Wynn-Thompson, T., Yazdi, M.N., 2019. Simulation of watershed-scale practices for mitigating stream thermal pollution due to urbanization. Sci. Total Environ. 671, 215–231.
Logan, L.H., Stillwell, A.S., 2018. Probabilistic assessment of aquatic species risk from thermoelectric power plant effluent: incorporating biology into the energy-water nexus. Appl. Energy 210, 434–450.
Loheide, S.P., Gorelick, S.M., 2006. Quantifying stream-aquifer interactions through the analysis of remotely sensed thermographic profiles and in situ temperature histories. Environmental Science & Technology 40 (10), 3336–3341.
Mazrooei, A., Sinha, T., Sankarasubramanian, A., Kumar, S., Peters-Lidard, C.D., 2017. Decomposition of sources of errors in seasonal streamflow forecasting over the U.S. Sunbelt. J. Geophys. Res. 120 (23), 11809–11825.
Mika, K., Gallo, E., Read, L., Edgley, R., Truong, K., Hogure, T.S., Pincetl, S., Gold, M., 2017. LA Sustainable Water Project: Los Angeles River Watershed. UCLA Institute of the Environment and Sustainability, p. 144.
Mohseni, O., Stefan, H.G., Erickson, T.R., 1998. A nonlinear regression model for weekly stream temperatures. Water Resour. Res. 34 (10), 2685.
Mongolo, J., Trusso, N., Dagit, R., Aguilar, A.A., Drill, S.L., 2017. A Longitudinal Temperature Profile of the Los Angeles River from June through October 2016: Establishing a Baseline. Southern California Academy of Sciences, p. 26.
Mosleh, L., Zamani-Miandashti, N., 2013. An investigation of objectives and problems of Shiraz green belt. Int. J. Adv. Biol. Biomed. Res. 1 (10), 1246–1252.
Moyle, P.B., Katz, J.V.E., Quinones, R.M., 2011. Rapid decline of California's native inland fishes: a status assessment. Biol. Conserv. 144, 2414e2423.
Nichols, A.L., Willis, A.D., Jeffres, C.A., Deas, M.L., 2014. Water temperature patterns below large groundwater springs: management implication for Coho Salmon in the Shasta River, California. River Res. Appl. 30, 442–455.
Nguyen, T.T.N., Némery, J., Gratiot, N., Strady, E., Quoc Tran, V., Truong Nguyen, A., Aimé, J., Peyne, A., 2019. Nutrient dynamics and eutrophication assessment in the tropical river system of Saigon - dongnai (Southern Vietnam). Sci. Total Environ. 653, 370–383.
Null, S.E., Mouzon, N.R., Elmore, L.R., 2017. Dissolved oxygen, stream temperature, and fish habitat response to environmental water purchases. J. Environ. Manag. 197, 559–570.
Ohio EPA, 2019. Nonpoint source program - permitting guidance for stream restoration projects. accessed at: https://www.epa.state.oh.us/portals/35/nps/319DOCS/FINAL%20Stream%20Restoration%20Permitting%20GUIDANCE%2001-07.pdf.
Pretty, J.N., Mason, C.F., Nedwell, D.B., Hine, R.E., Leaf, S., Dils, R., 2003. Environmental costs of freshwater eutrophication in England and Wales. Environ. Sci. Technol. 37 (2), 201–208.
Read, L.K., Hogue, T.S., Edgley, R., Mika, K.B., Gold, M., 2019. Evaluating the impacts of stormwater management on streamflow regimes in the Los Angeles River. J. Water Resour. Plan. Manag. 145 (10), 05019016.
Rheinheimer, D.E., Null, S.E., Lund, J.R., 2015. Optimizing selective withdrawal from reservoirs to manage downstream temperatures with climate warming. J. Water Resour. Plan. Manag. 141 (4), 04014063.
Risley, J.C., Constantz, J., Essaid, H., Rounds, S., 2010. Effects of upstream dams versus groundwater pumping on stream temperature under varying climate conditions. Water Resour. Res. 46 (6).
Roth, T.R., Westhoff, M.C., Huwald, H., Huff, J.A., Rubin, J.F., Barrenetxea, G., Parlange, M.B., 2010. Stream temperature response to three riparian vegetation scenarios by use of a distributed temperature validated model. Environ. Sci. Technol. 44 (6), 2072–2078.
Shafiei Shiva, J., Chandler, D.J., Kunkel, K.E., 2019. Localized changes in heatwave properties across the USA. Earth's Future 7. https://doi.org/10.1029/2018EF001085.
Seedang, S., Fernald, A.G., Adams, R.M., Landers, D.H., 2008. Economic analysis of water temperature reduction practices in a large river floodplain: an exploratory study of the Willamette River, Oregon. River Res. Appl. 24, 941–959.
Somers, K.A., Bernhardt, E.S., Grace, J.B., Hassett, B.A., Sudduth, E.B., Wang, S., Urban, D.L., 2013. Streams in the urban heat island: spatial and temporal variability in temperature. Freshw. Sci. 32 (1), 309–326.
Stefan, H.G., Sinokrot, B.A., 1993. Projected global climate change on water temperatures in five north-central U.S. streams. Clim. Change 24, 353–381.
Sun, N., Yearsley, J., Voisin, N., Lettenmaier, D.P., 2015. A spatially distributed model for the assessment of land use impacts on stream temperature in small urban watersheds. Hydrol. Process. 29 (10), 2331–2345.
US Army Corps of Engineers, 2016. HEC-RAS River Analysis System Hydraulic Reference Manual Version 5.0, CPD-68. US Army Corp of Engineers, Hydrologic engineering center, p. 960.
US Army Corps of Engineers, 2015. Los Angeles River Ecosystem Restoration Feasibility Study. U.S. Army Corps of Engineers, Los Angeles District, p. 623.
US Army Corps of Engineers, 2019. Los Angeles River Ecosystem Restoration Project. https://www.spl.usace.army.mil/Missions/Civil-Works/Projects-Studies/Los-Angeles-River-Ecosystem-Restoration/.
U.S. Geological Survey, 2016. The StreamStats Program online at. http://streamstats.usgs.gov. accessed on (Date of access:2019).
USDA-NRCS, 2007. National Engineering Handbook - Part 654 Stream Restoration Design Washington, DC, vol 6. United States Department of Agriculture, Natural Resources Conservation Service, pp. 6–36.
US EPA, 2013. EPA periodic retrospective review of existing regulations; Reducing Reporting Burden under Clean Water Act Sections 303 (D) and 305 (B), vol 303. U.S. Environmental Protection Agency, p. 68.
US EPA, 2016. Community Solutions for Stormwater Management, A Guide for Voluntary Long-Term Planning. U.S. Environmental Protection Agency Office of Water, p. 16. www.epa.gov/npdes/stormwater-planning.
Walsh, C.J., Roy, A.H., Feminella, J.W., Cottingham, P.E., Groffman, P.M., 2005. The urban stream syndrome: current knowledge and the search for a cure. J. North Am. Benthol. Soc. 24.
Weng, Q., Fu, P., 2014. Modeling annual parameters of clear-sky land surface temperature variations and evaluating the impact of cloud cover using time series of Landsat TIR data. Remote Sens. Environ. 140, 267–278.
Yang, Y., Endreny, T.A., Nowak, D.J., 2013. A physically based analytical spatial air temperature and humidity model. J. Geophys. Res. Atmos. 118, 1–15. https://lakestewardsofmaine.org/wp-content/uploads/2014/01/Maximum-Dissolved-Oxygen-Concentration-Saturation-Table.pdf.